An Improved Neural Network SC_MRAS Speed Observer in Sensorless Control for Six Phase Induction Drives

NGOC THUY PHAM[1], DIEP PHU NGUYEN[1], KHUONG HUU NGUYEN[2]
[1] Dept. of Electrical Engineering Technology, Industrial University of Ho Chi Minh City
[2]Dept. of TE and Electrical Engineering, Ho Chi Minh City University of Transport
Ngocpham1020@gmail.com; Diepphunguyeniuh@gmail.com;
Nguyenhuukhuonghcmutrans@gmail.com

Abstract: - During the recent decades there has been considerable development of sensorless vector controlled SPIM drives for high performance industrial applications. Sensorless drives have been successfully applied for medium and high speed operation, however, at low and zero speed operation, the instability and the poor performance of observers is still always a large challenge. In this paper, a novel Stator Current Based Model Reference Adaptive System (SC_MRAS) speed observer is proposed to improve the performance of the MRAS speed observer, especially at low speed region. In the new MRAS method, a two-layer linear Neural Network (NN), which has been trained online by means of an Ordinary Least quares (OLS) algorithm, is used as an adaptive model to estimate the stator current. The proposed algorithm is less complicated, reduce computational effort, the proposed observer are quicker convergence in speed estimation. It can ensure that the whole drive system achieves faster satisfactory torque and speed control and strong robustness, especially at low and zero speed region. Beside the adaptive model of the proposed scheme is employed in prediction mode also is a new point to make the proposed observer operate better accuracy and stability both in transient and steady-state operation, the dynamic performance is significantly improved. In this proposed, the rotor flux, which is needed for the stator current estimation of the adaptive model, is identifier by the Voltage Model (VM). Detailed simulations and experimental tests are carried out to investigate the performance of the proposed schemes when compared to the BPN MRAS. The results presented for the new scheme show the great improvement in the performance of the MRAS observer in sensorless modes of operation, especially at low and zero speed.

Key-Words: - Neural network; Sensorless vector control; Six phase induction motor drive; MRAS observer

1. Introduction

In recent decades, the multiphase motors have been proposed by the authors [1]. The main advantages of multiphase motors are higher torque density, greater efficiency, reduced torque pulsations, fault tolerance, and reduction in the required rating per inverter leg [1]. Therefore, multiphase motors are often considered in some applications such as locomotive traction, electrical ship propulsion, in high power applications such as automotive, aerospace, military and nuclear [2]. With its reliable working characteristics and high failure tolerance nowadays, this motors are even considered in the small power applications requiring high reliability and fault tolerance, where are expected that the loss of one or more phases the machine still can provide a significant electromagnetic torque to continue operating the system. Among the many types of multiphase motors, SPIM is one of the most widely used multiphase motors.

The high performance SPIM drives require the rotor speed information. This can be obtained through a speed sensor or be estimated through the values of stator voltage and current. The use of speed sensor is associated with problems as reduction of reliability and mechanical robustness of the drives and cost increase, need of shaft extension and injects noise into the system. Moreover, in certain applications it is difficult to mount sensors. Therefore, different techniques for the speed sensorless control of induction motors have been proposed. They usually are divided into two categories, the fundamental model based observers and anisotropies model based observers. Model-based estimation strategies include open-loop observers [3], sliding-mode observers [4], extended and unscented Kalman filters [5], model reference adaptive systems (MRAS) [6–7] and artificial intelligence (AI) [8]. Recent research also used predictive current control for sensorless IM drives [9]. The main drawback of these model based observers are their insufficient performance at low speeds and machine parameter sensitivity. In order to overcome these problems a high frequency voltage or current carrier were injected, needed to excite the saliency itself [10]. A different approach lies in trying to track the rotor slotting effect directly, without any high frequency carrier excitation [11]. These methods work well at low and near zero speed region. However, their major disadvantages are computational complexity, the need of external hardware for signal injection and the adverse effect of injecting signal on the machine performance. Therefore, because of its simplicity and ease of implementation the model based methods and especially MRAS based methods are, until now, the most widely used.

There are the different techniques to estimating the rotor speed for the high performance IM drives have been proposed. However, because of relatively simpler to implement and often requiring lower computational effort the MRAS schemes are, until now, the most widely used. The MRAS schemes have been proposed in the literature based on rotor flux proposed by Schauder Rotor-flux (RF-MRAS) [12]. This scheme suffers from DC drift problems associated with pure integration and sensitivity to stator resistance variations, especially in the low speed regions. The back-EMF MRAS scheme was introduced to overcome the pure integration problem [13]. However, this scheme is difficult to design its adaptation gain constants and sensitive to stator resistance variations. The reactive power MRAS (RP-MRAS) scheme is immune to stator resistance variations but its disadvantage is instability in regenerating mode [14]. Another approach, the stator current MRAS scheme has been introduced by the authors for the speed identification of induction motor (IM) drives [15]. Simulation and experimental results have showed that the significantly improvement in low speed operation performance. In the [16]–[17] present a stator current based MRAS speed observer using NN, which is an evolution of [15]. As the MRAS observer in [15] measured stator current components are used as the reference model to avoid the use of a pure integrator and reduce influence of motor parameter variation. However in the adaptive model, by rearranging the rotor equations of the machine so that a two-layer NN can be employed. A BPN algorithm for the online training of the NN to estimate the rotor speed. In [17], the observer is verified thought simulation and experiment, the lowest speed limit of the observer and the zero-speed operation, at no load and at load are presented. However, in [17] the use of the nonlinear BPN algorithm to training a neural network causes some problem as local minima, paralysis of the neural network, need of two heuristically chosen parameters, initialization problems, and convergence problems. The adaptive model in [17] is used in simulation mode, which means that its outputs are fed back recursively, this make reduce the accuracy and stability of the responses of observer.

With the aim to improve the performance of the MRAS speed observer based stator current presented in [17], a new scheme is proposed in this paper. In this proposed speed observer, the reference model uses the stator current components to free of pure integration problems and insensitive to motor parameter variations. The adaptive model based on the modified Euler integration has been used to solve the instability problems due to the discretization of the rotor equations of the machine. A linear neural network is used and trained online by means of an OLS algorithm instead of a nonlinear BPN algorithm to reduce the computation effort and overcome some drawbacks, which cause by its inherent nonlinearity. In addition, the adaptive model based on NN is implemented in the prediction mode instead of the simulation mode as in [17]. This ensures the proposed observer operate better accuracy and stability. In the proposed scheme, the rotor flux, which is needed for the stator current estimation of the adaptive model, is identifier by the Voltage Model (VM). The comparison between the proposed observer and the BPN SC MRAS observer has been implemented though simulation. Simulation results are given to compare the performance of the proposed BNP MRS observer [17]. The comparison data have proven that the proposed OLS_SC_MRAS observer are quicker convergence in speed estimation, better dynamic performances; lower estimation errors both in transient and steady-state operation. The terms of accuracy and robustness of the OLS_SC_MRAS observers is higher.

The paper is organized into five sections. In Section 2, the basic theory of the model of the SPIM and the SPIM drive are presented. Section 3 introduces the proposed OLS_ SC_ MRAS speed observer. Simulation and discuss are presented in Section 4. Finally, the concluding is provided in Section 5.

2. Model Vector Control Of Spim Drives

2.1 Model vector control of SPIM drives

The system under study consists of an SPIM fed by a six-phase VSI (voltage Source Inverter) and a DC link. A detailed scheme of the drive is provided in Fig.1. This SPIM is a continuous system that can be described by a set of differential equations. The model of the system can be simplified by means of the vector space decomposition (VSD). By applying this technique, the original six-dimensional space of the machine is transformed into three two-dimensional orthogonal subspaces in the stationary reference fame (α-β), (x-y) and (zl -z2). This transformation is obtained by means of 6 x 6 transformation matrix Eq (1).

$$T_6 = \begin{bmatrix} 1 & \frac{\sqrt{3}}{2} & -\frac{1}{2} & -\frac{\sqrt{3}}{2} & -\frac{1}{2} & 0 \\ 0 & \frac{1}{2} & \frac{\sqrt{3}}{2} & \frac{1}{2} & -\frac{\sqrt{3}}{2} & -1 \\ 1 & -\frac{\sqrt{3}}{2} & -\frac{1}{2} & \frac{\sqrt{3}}{2} & -\frac{1}{2} & 0 \\ 0 & \frac{1}{2} & -\frac{\sqrt{3}}{2} & \frac{1}{2} & \frac{\sqrt{3}}{2} & -1 \\ 1 & 0 & 1 & 0 & 1 & 0 \\ 0 & 1 & 0 & 1 & 0 & 1 \end{bmatrix} \quad (1)$$

In that, an amplitude invariant criterion was used. From the motor model obtained by using the VSD approach, the following conclusions should be emphasized:

1. The electromechanical energy conversion variables are mapped to the (α-β) subspace. The non-electromechanical energy conversion variables can be found in other subspaces.
2. The current components in the (x-y) subspace do not contribute to the air gap flux so they should be controlled to be as small as possible.
3. The voltage vectors in the (zl -z2) are zero due to the separated neutrals configuration of the machine.

A VSI has a discrete nature, actually, it has a total number of different switching states defined by six switching functions corresponding to the six inverter legs [Sa,Sx,Sb,Sy,Sc,Sz], where Si ϵ {0,1}. On the other hand, a transformation matrix must be used to represent the stationary reference fame (α-β) in the dynamic reference (d - q). This matrix is given:

$$T_{dq} = \begin{bmatrix} \cos(\delta_r) & -\sin(\delta_r) \\ \sin(\delta_r) & \cos(\delta_r) \end{bmatrix} \quad (2)$$

The different switching states and the voltage of the DC link define the phase voltages which can in turn be mapped to the (α-β) - (x-y) space according to the Vector space decomposition VSD approach.

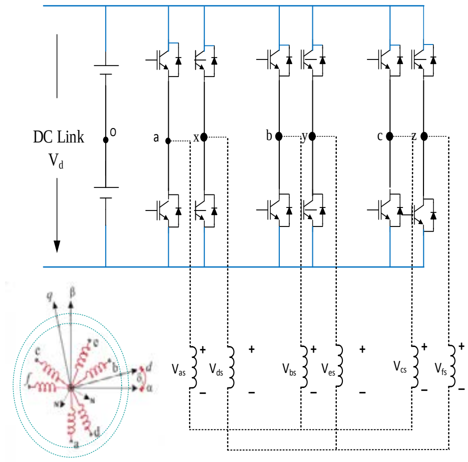

Fig.1 A general scheme of an SPIM drive

Fig.2 Switching states in (α-β) and (x-y) subspaces for a SP VSI

2.2 Model of SPI

In this part a six phase induction motor, which contains two sets of three phase winding spatially shifed by 30 electrical degrees with isolated neutral points (as depicted in Fig. 1), is modeled. Stator and rotor voltage equation for this model is as follows:

$$[V_s] = [R_s][I_s] + P([L_s][I_s] + [M][I_r] \quad (3)$$

$$[V_r] = [R_r][I_r] + P([L_r][I_r] + [M][I_s] \quad (4)$$

where: [V], [I], [R], [L] and [M] are voltage, current, resistant, self and mutual inductance vectors, respectively. P is differential operator. Subscript r and s related to the rotor and stator resistance respectively. Since the rotor is squirrel cage, [Vr] is equal to zero. By this matrix, the six-dimensional system is transferred to three orthogonal two dimensional subspaces (α-β), (x, y), (z1, z2), Stator and rotor equations in these different subspaces can be stated as: (α-β), (x, y), (z1, z2) subspaces :

$$\begin{bmatrix} V_{s\alpha} \\ V_{s\beta} \\ 0 \\ 0 \end{bmatrix} = \begin{bmatrix} R_s + PL_s & 0 & PM & 0 \\ 0 & R_s + PL_s & 0 & PM \\ PM & \omega_r M & R_r + PL_r & \omega_r M \\ -\omega_r M & PM & -\omega_r M & R_r + PL_r \end{bmatrix} \begin{bmatrix} I_{s\alpha} \\ I_{s\beta} \\ I_{r\alpha} \\ I_{r\beta} \end{bmatrix}$$

$$\begin{bmatrix} V_{sx} \\ V_{sy} \\ 0 \\ 0 \end{bmatrix} = \begin{bmatrix} R_s + PL_s & 0 & 0 & 0 \\ 0 & R_s + PL_s & 0 & 0 \\ 0 & 0 & R_r + PL_r & 0 \\ 0 & 0 & 0 & R_r + PL_r \end{bmatrix} \begin{bmatrix} I_{sx} \\ I_{sy} \\ I_{rx} \\ I_{ry} \end{bmatrix}$$

(5)

$$\begin{bmatrix} V_{sz1} \\ V_{sz2} \\ 0 \\ 0 \end{bmatrix} = \begin{bmatrix} R_s + PL_s & 0 & 0 & 0 \\ 0 & R_s + PL_s & 0 & 0 \\ 0 & 0 & R_r + PL_r & 0 \\ 0 & 0 & 0 & R_r + PL_r \end{bmatrix} \begin{bmatrix} I_{sz1} \\ I_{sz2} \\ I_{rz1} \\ I_{rz2} \end{bmatrix}$$

where: $L_s=L_{ls}+M$, $L_r= L_{lr}+M$, $M=3.L_{ms}$, p=d/dt. As these equations implies, the electromechanical conversion, only takes place in the α-β subspace (DQ subspace) and the other subspaces just produce losses.

So the torque equation can be written as follows:

$$T_e = 3P(\psi_{rQ}\,\mathrm{i}_{rD} - \psi_{rD}\,\mathrm{i}_{rQ})$$

(6)

$$\mathrm{j}_i \frac{d}{dt}\omega_r + B_i\omega_r = P(T_e - T_L) \qquad (7)$$

where: respectively, Ji, ωr, Bi, Tm, TL, P are inertia coefficient, angular speed, fiction factor, the electromagnetic torque that generated by the motor, load torque, number of poles and stator flux linkage at the related subspace.

3. OLS NN_SC_MRAS speed observer

3.1 PI_SC_ MRAS observer

In the classical rotor flux MRAS speed observer, the reference model, usually expressed as a Voltage Model (VM), represents the stator equation and can be written as following:

$$\frac{d\psi_{rD}}{dt} = \frac{x_r}{x_m}(v_{sD} - R_s i_{sD} - \sigma T_n x_s p i_{sD})$$
$$\frac{d\psi_{rQ}}{dt} = \frac{x_r}{x_m}(v_{sQ} - R_s i_{sQ} - \sigma T_n x_s p i_{sQ}) \qquad (6)$$

where: r_s: stator resistances, xs = xm + xsσ; xr = xm + xrσ; xm: respectively stator, rotor reactances and magnetizing, xσs, xσr: stator and rotor leakage reactances, p=d/dt; Tn = 1/2πfsn, σ = 1- xm2 /xs xr, fsn: nominal frequency.
The adaptive model, usually represented by the Current Model (CM), describes the rotor equation where the rotor flux components are expressed in terms of stator current components and the rotor speed.

$$\frac{d\psi_{rD}}{dt} = \frac{r_r}{x_r}(x_m i_{sD} - \psi_{rD}) - \omega\psi_{rQ})T_n$$
$$\frac{d\psi_{rQ}}{dt} = \frac{r_r}{x_r}(x_m i_{sQ} - \psi_{rQ}) - \omega\psi_{rD})T_n \qquad (7)$$

Looking at the formula (6), it is easy to find the presence of r_s and rotor flux, These make the traditional RF_MRAS observer suffered by pure integration problems, which being able to cause dc drift and initial condition problems, and insensitive to motor parameter variations. In order to overcome these problems another approach, the stator current MRAS scheme has been proposed, the stator current components is used as a reference model. The stator current estimator is adjustable model. The estimated stator current components are compared with their measured values, and the signal e_{is} is used in the adaptation mechanism (9) to generate the rotor speed. In this observer, the mathematical model of the stator current observer can be calculated from the combined voltage- and current models and is described by the following equation:

$$T_n \frac{d\hat{i}_{sD}}{dt} = \frac{1}{x_s\sigma}\left[v_{sD} - r_s i_{sD} - \frac{x_m}{x_r}(r_r \frac{x_m}{x_r} i_{sD} - \frac{r_r}{x_r}\psi_{r,D} - \omega\hat{\psi}_{r,Q})\right]$$
$$T_n \frac{d\hat{i}_{sQ}}{dt} = \frac{1}{x_s\sigma}\left[v_{sQ} - r_s i_{sQ} - \frac{x_m}{x_r}(r_r \frac{x_m}{x_r} i_{sQ} - \frac{r_r}{x_r}\psi_{r,Q} - \omega\hat{\psi}_{r,D})\right] \qquad (8)$$

The adjustable model (8) requires information about the rotor flux. This is calculated on the basis of voltage model (VM) (6) or current model (CM). In the PI_SC_MRAS observer, the used adaptation algorithm is based on the error between estimated and measured stator current developed in [18] (basing on the minimization of the Lyapunov function)

$$\hat{\omega}_r = k_p(e_{iD}\psi_{rQ} + e_{iQ}\psi_{rD}) + \frac{k_i}{p}(e_{iD}\psi_{rQ} + e_{iQ}\psi_{rD})dt \qquad (9)$$

where $e_{isD} = i_{sD} - i_{esD}$, $e_{isQ} = i_{sQ} - i_{esQ}$ is the error between estimated and measured stator current. The obtained rotor-speed value is used in the stator-current estimators as changeable parameter, as shown in the Fig.3

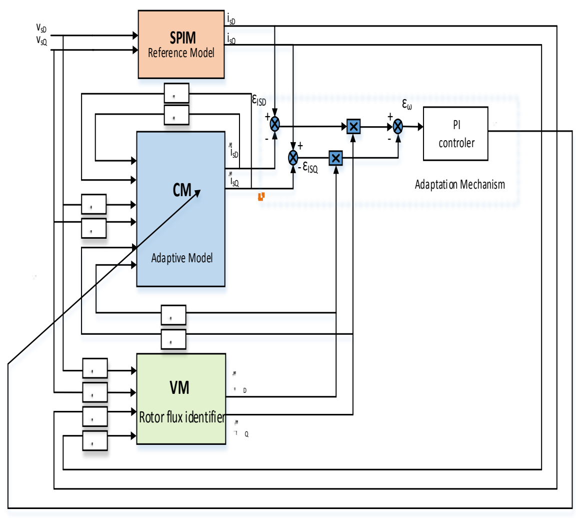

Fig.3 PI _SC_ MRAS speed observer

3.2 OLS NN_SC_ MRAS observer

3.2.1 Structure of the OLS_SC_ MRAS Observer

In this scheme, the measured stator current components are also used as the reference model of the MRAS observer to avoid the use of a pure integrator and reduce influence of motor parameter variation as in [15-17]. The adaptive model is a two-layer linear NN to estimate the stator current has been trained online by means of an ordinary least-squares (OLS) algorithm. This adaptive model is described by the combined voltage- and current models in the stator reference frame (8)

Eq. (8), Then they been divided by Tn, be re written in the following as:

$$\dot{X} = AX + Bu \tag{10}$$

where:

$$\dot{X} = \begin{vmatrix} \frac{di_{sD}}{dt} \\ \frac{di_{sQ}}{dt} \end{vmatrix}; X = \begin{vmatrix} i_{sD} \\ i_{sQ} \end{vmatrix}; A_x = \begin{bmatrix} -\left(1+\frac{x_m^2}{x_r^2}\right)\frac{r_s}{x_s\sigma} \\ -\left(1+\frac{x_m^2}{x_r^2}\right)\frac{r_s}{x_s\sigma} \end{bmatrix};$$

$$B_x = \begin{bmatrix} \frac{1}{x_s\sigma} & 0 & \frac{1}{x_s\sigma}\frac{r_r x_m}{x_r^2} & \frac{1}{x_s\sigma}\frac{\omega_r x_m}{x_r^2} \\ 0 & \frac{1}{x_s\sigma} & \frac{1}{x_s\sigma}\frac{\omega_r x_m}{x_r^2} & -\frac{1}{x_s\sigma}\frac{r_r x_m}{x_r^2} \end{bmatrix}; u_s = \begin{bmatrix} u_{sQ} \\ u_{sQ} \\ \psi_{rD} \\ \psi_{rQ} \end{bmatrix}$$

Its corresponding discrete model is, therefore, given by:

$$\hat{X}_{(k)} = e^{A_x T_s} i_{(k-1)} + \left[e^{A_x T_s} - I\right] A_x^{-1} B_x u_{s(k-1)} \tag{11}$$

$e^{A_x T_s}$: is generally computed by truncating its power series ex pansion, i.e.,

$$e^{A_x T_s} = I + \frac{A_x T_s}{1!} + \frac{A_x^2 T_s}{2!} + ... + \frac{A_x^n T_s}{n!} \tag{12}$$

If n=1, the simple forward Euler method is obtained, which gives the following finite difference equation [15-17]

$$\hat{i}_{sD(k)} = w_1 \hat{i}_{sD(k-1)} + w_2 u_{sD(k-1)} + w_3 \hat{\psi}_{rQ(k-1)} + w_4 \hat{\psi}_{rD(k-1)}$$
$$\hat{i}_{sQ(k)} = w_1 \hat{i}_{sQ(k-1)} + w_2 u_{sQ(k-1)} + w_3 \hat{\psi}_{rD(k-1)} + w_4 \hat{\psi}_{rQ(k-1)} \tag{13}$$

where marks the variables estimated with the adaptive model and is the current time sample. A neural network can reproduce these equations, where are the weights of the neural networks defined as:

$$w_1 = 1 - \frac{T_s r_s}{\sigma L_s} - \frac{T_s L_m^2}{\sigma L_s L_r T_r};\ w_2 = \frac{T_s}{\sigma L_s};\ w_3 = \frac{T_s L_m}{\sigma L_s T_r}; w_4 = \frac{T_s L_m \hat{\omega}_r}{\sigma L_s L_r} \tag{14}$$

where: $\hat{i}_s(k)$ is the current variables estimated with the adaptive model and k is the current time sample. An artificial neural network (ANN) can reproduce these equations, where w1, w2, w3, w4 are the weights of the neural networks defined as (14); Ts is the sampling time for the stator current observer. The ANN has, thus, four inputs and two outputs [16]–[17]. In the ANN, the weights w1, w2 and w3 are kept constant to their values computed offline while only w4 is adopted online. These equations are the same as those obtained in [17]. In the scheme is presented in [17], the adaptive model is characterized by the feedback of delayed estimated stator current components to the input of the neural network, which means that the adaptive model employed is in simulation mode. Moreover, the adaptive model is tuned online (training) by means of a BPN algorithm, however, nonlinear in its nature with the consequent drawbacks (local minima, heuristics in the choice of the network parameters, paralysis, convergence problems).

In this OLS_SC_MRAS observer proposed, the adaptive model based on the ADALINE has been improved, A linear least-square algorithm, which is more suitable than a nonlinear one, like the BPN, is used to reduce the computation effort and overcome some drawbacks, which cause by its inherent nonlinearity. Furthermore, the employment of the adaptive model in prediction mode leads to a quicker convergence of the algorithm, a higher bandwidth of the speed control loop, a better behavior at zero-speed, lower speed estimation errors both in transient and steady-state conditions.

An integration method more efficient than that used in (15) is the so-called modified Euler integration, which also takes into consideration the values of the variables in two previous time steps [19]. From (9), the following discrete time equations can be obtained, as shown in (15). Also, in this case, a neural network can reproduce these equations, where and are the weights of the neural networks defined as (16).

$$\hat{i}_{sD(k)} = w_1 i_{sD(k-1)} + w_2 u_{sD(k-1)} + w_3 \hat{\psi}_{rD(k-1)} + w_4 \hat{\psi}_{rQ(k-1)} + w_5 i_{sD(k-2)} - w_6 u_{sD(k-2)} - w_7 \hat{\psi}_{rD(k-2)} - w_8 \hat{\psi}_{rQ(k-2)}$$

$$\hat{i}_{sQ(k)} = w_1 i_{sQ(k-1)} + w_2 u_{sQ(k-1)} + w_3 \hat{\psi}_{rQ(k-1)} - w_4 \hat{\psi}_{rD(k-1)} + w_5 i_{sQ(k-2)} - w_6 u_{sQ(k-2)} - w_7 \hat{\psi}_{rQ(k-2)} + w_8 \hat{\psi}_{rD(k-2)}$$

where:
(15)

$$w_1 = 1 - \frac{3TR_s}{2\sigma L_s} - \frac{3TL_m^2}{2\sigma L_r L_s T_r};\ w_2 = \frac{3T}{2\sigma L_s};\ w_3 = \frac{3TL_m}{2\sigma L_r L_s T_r};\ w_4 = \frac{3TL_m}{2\sigma L_r L_s}\omega_r;$$
$$w_5 = \frac{3TR_s}{2\sigma L_s} + \frac{TL_m^2}{2\sigma L_r L_s T_r};\ w_6 = \frac{T}{2\sigma L_s};\ w_7 = \frac{TL_m}{2\sigma L_r L_s T_r};\ w_8 = \frac{TL_m}{2\sigma L_r L_s}\omega_r$$

(16)

Rearranging (15), the matrix equation is obtained in prediction mode; see (17). This matrix equation can be solved by any least-square technique. This is a classical matrix equation of the type, where A is called a “data matrix”, b is called an“observation vector,” and A is the scalar unknown, In this application a classical OLS algorithm in a recursive form has been employed; This algorithm is described in detail in [19,20]. Fig. 4 shows the block diagram of the OLS_SC_ MRAS speed observer.

$$\begin{bmatrix} \frac{3TL_m}{2\sigma L_r L_s}\hat{\psi}_{rQ(k-1)} - \frac{TL_m}{2\sigma L_r L_s}\hat{\psi}_{rQ(k-2)} \\ -\frac{3TL_m}{2\sigma L_r L_s}\hat{\psi}_{rD(k-1)} + \frac{TL_m}{2\sigma L_r L_s}\hat{\psi}_{rD(k-2)} \end{bmatrix} \omega_{r(k-1)} = \begin{bmatrix} \hat{i}_{sQ(k)} - w_1 i_{sQ(k-1)} - w_2 u_{sQ(k-1)} - w_3 \hat{\psi}_{rQ(k-1)} + w_5 i_{sQ(k-2)} + w_6 u_{sQ(k-2)} + w_7 \hat{\psi}_{rQ(k-2)} \\ \hat{i}_{sQ(k)} - w_1 i_{sQ(k-1)} - w_2 u_{sQ(k-1)} - w_3 \hat{\psi}_{rQ(k-1)} + w_5 i_{sQ(k-2)} + w_6 u_{sQ(k-2)} + w_7 \hat{\psi}_{rQ(k-2)} \end{bmatrix}$$

(17)

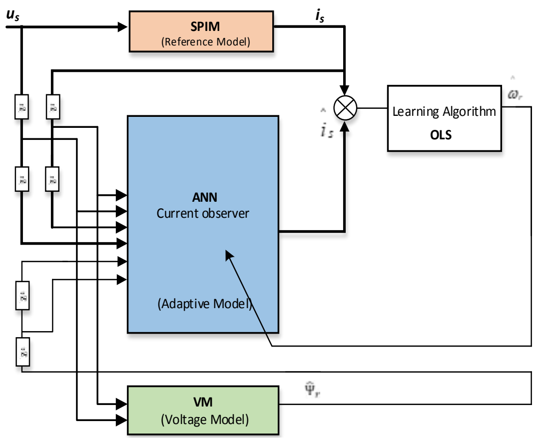

Fig.4 OLS_ SC_ MRAS speed observer

3.2.2 Rotor Speed Estimation Algorithm:

Ax ~ b is the linear regression problem under hand.

All LS problems have been generalized by using a parameterized formulation (generalized OLS) of an error function whose minimization yields the corresponding solution. This error is given by :

$$E_{OLS} = (Ax - b)^T (Ax - b) \tag{18}$$

where $(Ax - b) = \varepsilon = \begin{bmatrix} \varepsilon_{isD} \\ \varepsilon_{isQ} \end{bmatrix} = \begin{bmatrix} i_{sD}(k) - \hat{i}_{sD}(k) \\ i_{sQ}(k) - \hat{i}_{sQ}(k) \end{bmatrix}$

This error can be minimized with a gradient descent method:

$$\omega_r(k+1) = \omega_r(k) - \eta\gamma(k)\,a(k) \tag{19}$$

Where

$$\gamma(k) = a(k)^T a(k) - b(k) \tag{20}$$

where η is the learning rate, a(k) is the row of A fed at instant k, and b(k) is the corresponding observation.

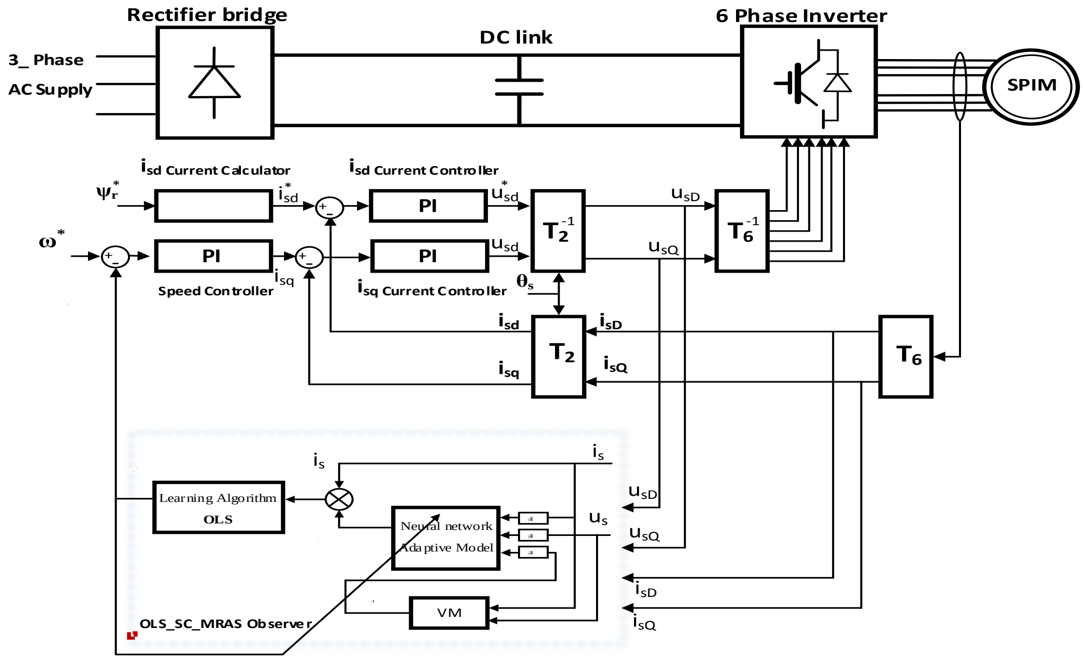

Fig.5 Sensorless vector control of SPIM drive using NN_SC_MRAS observer

4. Simulink and Discussion

To verify and evaluate the performance of the SC_MRAS using NN observer a sensorless vector control of SPIM drive system, as shown in Fig. 5 has been simulated at different speed ranges through Matlab simulation software, specially surveyed at low speed range. SPIM parameters: 1HP, 220 V, 50 Hz, 4 pole, 1450 rpm. Rs = 10.1Ω, Rr = 9.8546Ω, Ls = 0.833457 H, Lr = 0.830811H, m = 0.783106H, Ji = 0.0088 kg.m2.

4.1 Test 1: Dynamic Performance:

In this test, the improvements in terms of dynamic performance achieved with the OLS MRAS observer have been verified by comparing the speed responses of both proposed OLS_SC_MRAS and BPN_SC_MRAS observer during second speed reversals, respectively, from 100 to 100 rad/s, from 50 to 50 rad/s.

Fig. 6(a) (b) and Fig. 7(a) (b) show the reference, estimated, measured speed and the speed error during speed reversal. The simulation results show that for the OLS_SC_MRAS: The speed estimation convergence is faster, the speed estimation error is lower than the corresponding one obtained with the BPN MRAS.

In during speed transients the dynamic performance is better and the estimation error is lower, the maximum overshoot obtained with the OLS MRAS is lower than the corresponding one with the BPN MRAS because of the absence offiltering of the estimated stator current in the OLS_SC_MRAS observer.

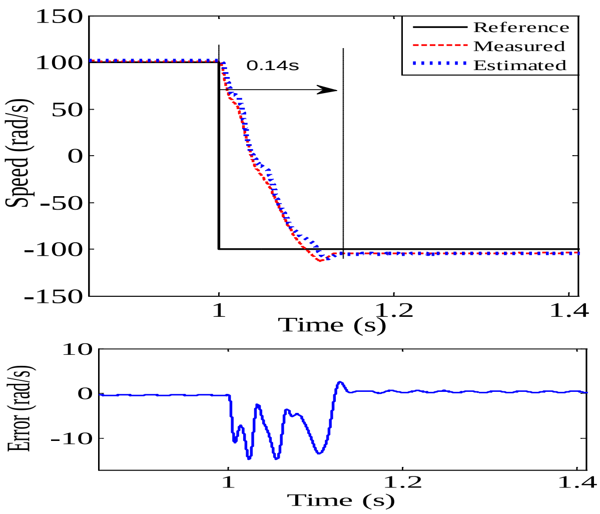

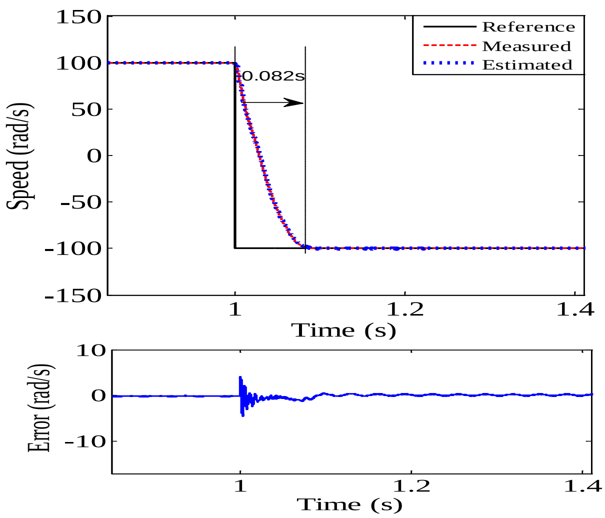

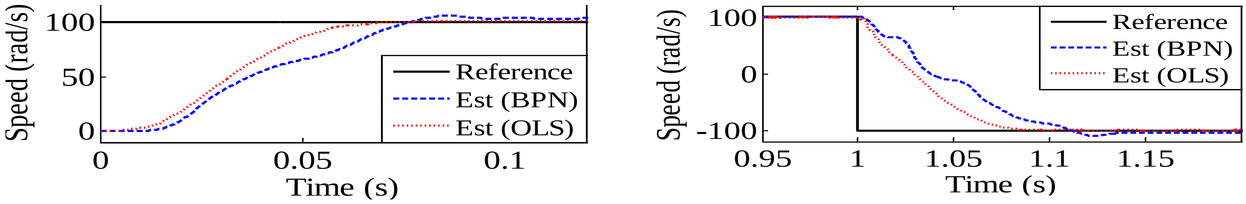

Fig.6 Estimated and measured speed and speed error and speed error during a speed reversal from 100 to -100 rad/s, (a) BPN MRAS observer; (b) OLS MRAS observer.

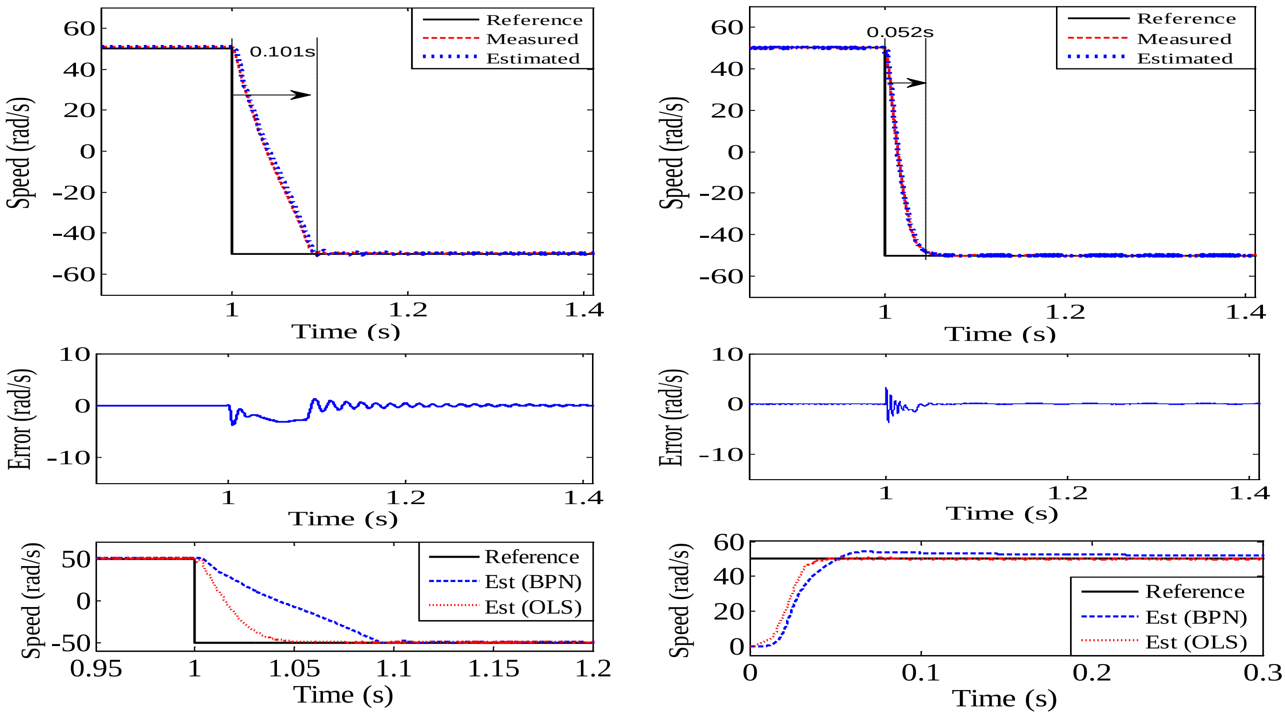

Fig.7 Estimated and measured speed and speed error and speed error during a speed reversal from 50 to -50 rad/s, (a) BPN MRAS observer; (b) OLS MRAS observer.

4.2 Test 2: The performance of proposed observer in medium and low speed ranges:

The performance of the proposed speed observer in the medium and low speed ranges was verified by providing different speed reference rates range from 100 rad/s to 30 rad/s and working with rated load. This simulation was performed with two sets of observations using OLS_SC_MRAS and BPN_SC_MRAS for comparison, evaluation the performance of both. The Fig.8 a,b shows the reference speed, estimated speed, actual speed and speed error of OLS_SC_MRAS and BPN_SC_MRAS observer, respectively.

The simulation results clearly show that the estimation accuracy in the medium and low speed range is very good, with negligible estimation errors during steady state and very low instantaneous estimation errors during the speed transients. Similar results have been obtained with the BPN MRAS observer: they presented, as a difference, only a slightly higher instantaneous estimation error, as explained in Test 1.

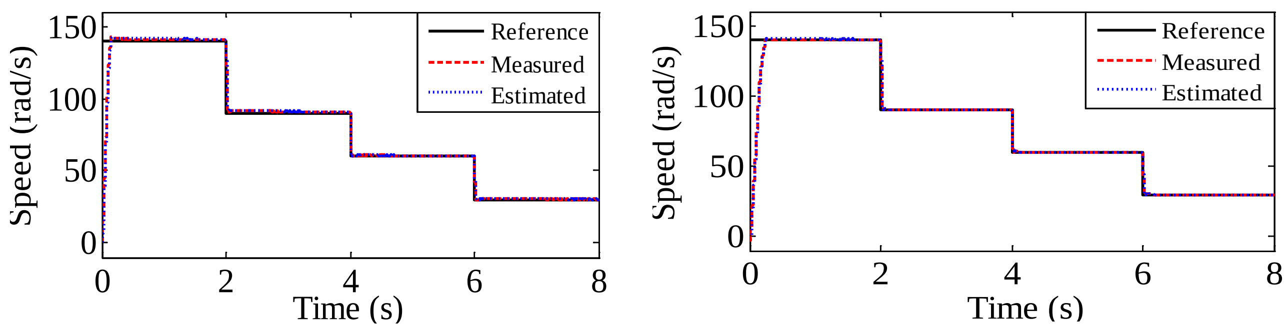

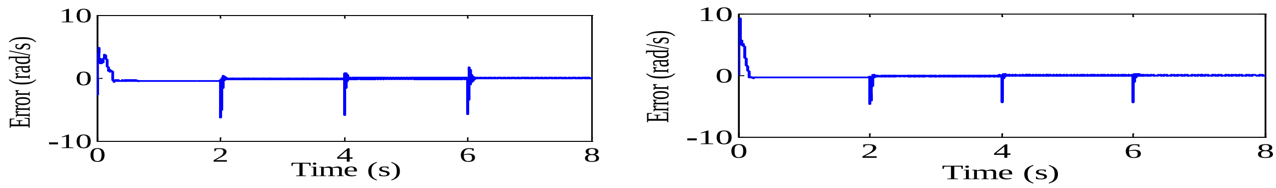

Fig.8 Reference, estimated. measured speed and speed error during a series of speed steps with rated load, (a) BPN MRAS observer. (b) OLS MRAS observer

4.3 Test 3: The performance of proposed observer in very low speed ranges:

In this three test, the performance of the speed estimation has been verified in the very low and zero speed ranges, by providing the sets of diffrrent speed reference ranges from 0 to 5 rad/s with each step the change is 1 rad/s working with 50% rated load.

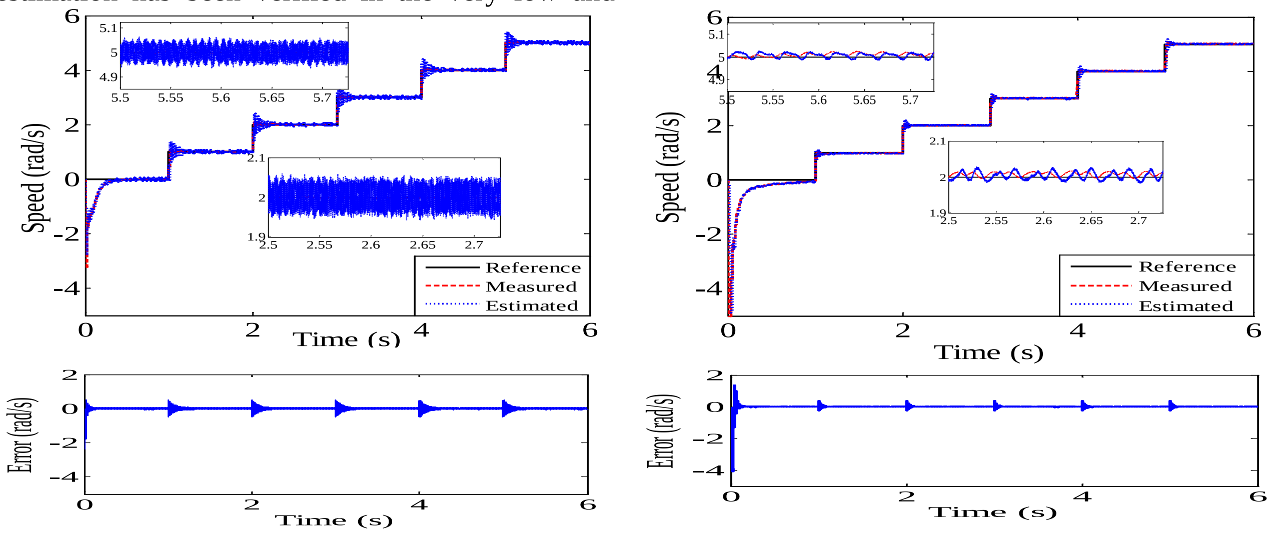

Fig.9 The speed of the SPIM in very low operation speed region using:
a. the OLS MRAS observer; b. the BPN MRAS observer

In any case, better results in the estimation accuracy at low speeds are to be expected with both OLS MRAS and BPN MRAS observers because the SPIM itself is used as reference model so the SC_MRAS observer free free from stator resistance dependency and dc drift problems, this is help to improve the performance of the observer specially at low speeds. The steady-state percent speed estimation error obtained with the OLS_ SC_MRAS observer is better than that with the RF_ MRAS observer, where the reference model uses the VM, is dependent on the stator stator and the pure integration. The speed estimation error is improved slightly than BPN_SC_MRAS, as explained in Test 1. These results in Fig. 9 show that, with both speed observers, the steady-state speed estimation error obtained with the OLS MRAS observer is slightly lower than that with the BPN_SC_MRAS. Fig. 10 show that stator current and rotor flux responses at low speed (5 rad/s) are quite accurate.

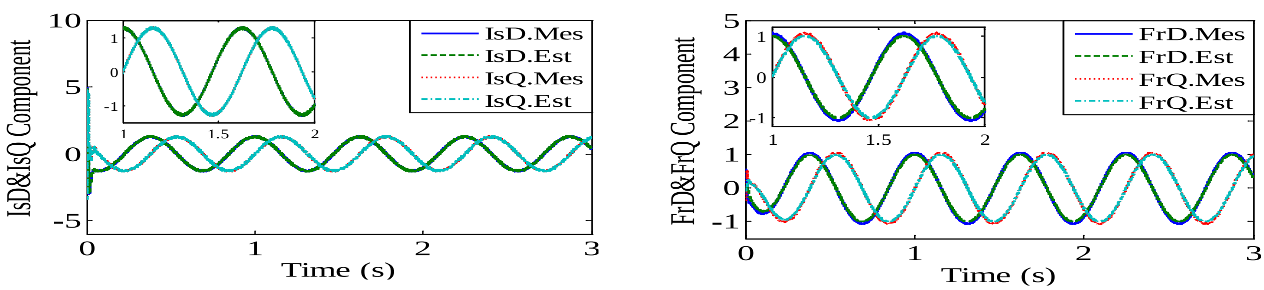

Fig.10 The stator current and rotor flux components when using the OLS MRAS observer at 5rad/s.

4.4 Test 4: Load Perturbations.

In this test, the robustness of the speed estimation to a sudden torque perturbation has been surveyed. It was carried out to prove the robustness of speed observer under variable load torque. For this test the rotor speed was kept constant at 1.5 rad/s with the torque applied +/- 50% rated torque.

Fig. 11a b show the speed and torque responses of the SPIM drive. These results show that the speed responses of the drive using the proposed OLS SC_MRAS observer occurs immediately when the torque steps are applied. Even during the speed transient that caused by the torque step, the estimated speed follows the real speed is very good. The simulation results show that the speed estimation convergence of the OLS_SC_MRAS observer is faster than that obtained with the BPN SC_MRAS observer.

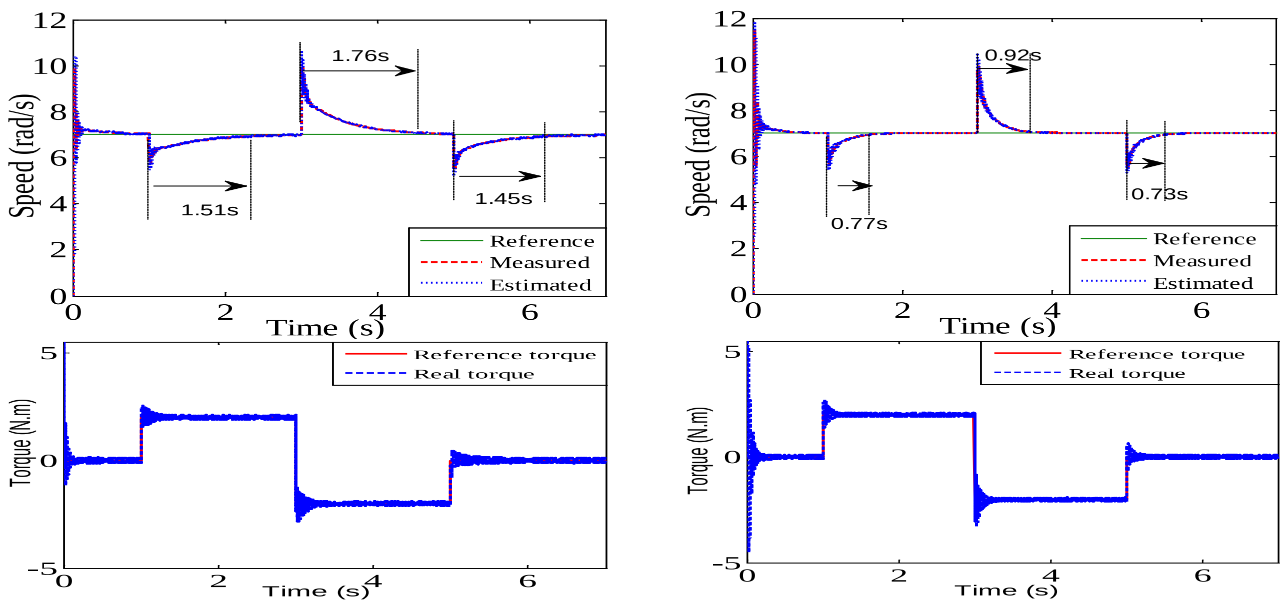

Fig.11 The speed with +/-50% load disturbance rejection of the drive using: a. the OLS MRAS observer; b. the BPN MRAS observer.

5. Conclusion

This paper has presented a OLS_ SC_MRAS speed observer for high performance SPIM drives using neural networks. It lead evoluting and improving the MRAS observer shown in [17]. The new SC_MRAS speed observer uses the CM discretized with the mopdified Euler integration method to solve the instability problems due to the discretization of the rotor equations of the machine. Then reagraning a linear neural network is used and trained online by means of an OLS algorithm instead of a nonlinear BPN algorithm, which is heavier from the complexity and computational burden and its inherent nonlinearity also cause some disadvantages as local minima, two heuristically chosen parameters, initialization, and convergence problems, paralysis of the neural network. In addition, the adaptive model based on NN is implement in prediction mode instead of simulation mode as in [17]. This ensures the proposed observer operate better accuracy and stability. The simulation results shown that the proposed observer are quicker convergence in speed estimation, better dynamic performances; lower estimation errors both in transient and steady state operation; better operation zeroand low speed region.

References

[1] E. Levi, Multiphase electric machines for variable-speed applications, *IEEE Transactions on Industrial Electronics*. 2008, 55(5), 1893 – 1909.

[2] R. Kianinezhad, B. Nahid-Mobarakeh, L. Baghli, F. Betin, G.A. Capolino, Modeling and Control of Six-Phase Symmetrical Induction Machine Under Fault Condition Due to Open Phases, *IEEE Trans. Ind. Elec.*, 2008,55 (5), 1966-1977.

[3] Kubota, H., Matsuse, K., Nakano, DSP-based speed adaptive flux observer of induction motor, *IEEE Trans. Ind. Appl.*, 1993, 29, (2), 344–348.

[4] Tak R, Kumar SY, Rajpurohit BS, Parameter Compensation of Induction Motor Drives using Second order of Sliding Mode Controller, *WSEAS Transactions on Ssystems and Control*, 2018, Vol.13.

[5] Jafarzadeh, S., Lascu, C., Fadali, State estimation of induction motor drives using the unscented Kalman filter, *IEEE Trans. Ind. Electron.*, 2012, 59(11), 4207–4216

[6] Liu X , Zhang G, Mei L, and Wang D, Speed Estimation and Parameters Identification Simultaneously of PMSM Based on MRAS, *WSEAS Transactions on Ssystems and Control, 2017, Vol.12.*

[7] Urbanski K, A New Sensorless Speed Control Structure For PMSM Using Reference Model, *Bulletin of the Polish Academy of Sciences Technical Sciences, 2017, 65(4), 489 – 496.*

[8] Maiti, S. Verma, V. Chakraborty, C. Hori, An adaptive speed sensorless induction motor drive with artificial neural network for stability enhancement, *IEEE Trans. Ind. Inf.*, 2012, 8, (4), 757–766

[9] *Yaman B. Zbede, Shady M. Gadoue, and David J. Atkinson, "Model Predictive MRAS Estimator for Sensorless Induction Motor Drives, IEEE Trans. Ind. Electronics. 2016, 63 (6), 3511*

[10] Foo G, Rahman, Sensorless sliding-mode MTPA control of an IPM synchronous motor drive using a sliding-mode observer and HF signal injection, *IEEE Trans. Ind. Electron.* 2010, 57(4), 1270-1278.

[11] Keysan, O. Ertan, Real-Time Speed and Position Estimation Using Rotor Slot Harmonics, *Industrial Informatics, IEEE Transactions on*. 2013, 9(2), 899-908.

[12]C. Schauder. Adaptive speed identification for vector control of induction motors without rotational transduce. IEEE Trans. Ind. Appl., 1992, 28(5), 1054–1061.

[13] Rashed, M., Stronach, A stable back-EMF MRAS-based sensorless low speed induction motor drive insensitive to stato resistance variation, *IEE Proc. Electr. Power Appl.,* 2004, 151, (6). pp. 685–693

[14] Peng, F., Fukao, Robust speed identification for speed-sensorless vector control of induction motors, *IEEE Trans. Ind. Appl.*, 1994, 30, (5), pp. 1234–1240.

[15] Gadoue, S.M., Giaouris, D., Finch, A neural network based stator current MRAS observer for speed sensorless induction motor drives, *Proc. IEEE Int. Symp. Industrial Electronics, UK,* 2008, pp. 650–655

[16] Gadoue, S.M., Giaouris, D., Finch, J.W, An experimental assessment of a stator current MRAS based on neural networks for sensorless control of induction machines, *Sensorless Control for Electrical Drives, Birmingham, UK,* 2011, pp. 102–106

[17] Shady M. Gadoue, Damian Giaouris and John W. Finch, Stator current model reference adaptive systems speed estimator for regenerating-mode low-speed operation of sensorless induction motor drives, *IET Electric Power Applications*, 2013, 7(7), 597–606.

[18] Teresa Orlowska-Kowalska, and Mateusz Dybkowski, Stator-Current-Based MRAS Estimator for a Wide Range Speed-Sensorless Induction-Motor Drive, *IEEE Transactions On Industrial Electronics*, 2010, 57(4), 1296-1308.

[19] J. H. Matheus and K. D. Fink, Numerical Methods Using Matlab 4th ed. *Upper Saddle River, NJ: Prentice-Hall*, 2004.

[20]G. Cirrincione, M. Cirrincione, J. Hérault, and S. Van Huffel, The MCA EXIN neuron for the minor component analysis: Fundamentals and comparisons, *IEEE Trans. Neural Netw.*, 2002, 13(1), pp. 160–187.